CHAPTER 7

MODELING AND PREDICTION OF SPATIO-TEMPORAL LAND USE AND LAND COVER DYNAMICS USING GEOSPATIAL TECHNIQUE

7.1 INTRODUCTION

The analysis and monitoring of LULC changes (LULCC) are vital for understanding complex interactions between human activities and global environmental changes (Dickinson, 1995; Zhu and Woodcock, 2014). LULCC mainly focuses on spatio-temporal dynamics and the human interferences largely influence the earth's environment by changing the dynamics of LULC (Thies et al., 2014). With the growing population and increasing socio-economic requirements, a pressure is created on LULC which leads to changes in it in a spontaneous and uncontrolled manner (Seto et al., 2002). Therefore, with increasing LULCC, mainly because of human activities, it is essential to identify such changes, appraisal of their trends and effects on the environment and ecosystem for future planning and natural resource management (Prenzel, 2004).

In several studies, the integration of RS and GIS served as an efficient scheme for analyzing and detecting the spatial allocation of changes in LULC over large areas (Carlson and Azofeifa, 1999; Shooshtari and Gholamalifard, 2015; Waiyasusri et al., 2016). In recent years, the spatio-temporal modeling of LULC dynamics has drawn a lot of attention in solving the problems that occur due to the alteration and conversion of LULC (Lambin et al., 2001).The studies of modeling approaches for future scenarios depend on predictions, whereas the analyses and reviews of the past to the current depend on facts. However, the

prediction of future situation is directly linked to the changes detected from the past to the current as well (Bhatta, 2010).

It is necessary to apply spatially explicit models to simulate and predict the changes in LULC with the purpose to appraise future scenarios. Consequently, accurate and timely information provided by RS technologies at regular interval can be applied efficiently to detect and analyze the past and current trends as well as to predict future trends of LULC (Dadhich and Hanaoka, 2011; Mishra et al., 2014; Mishra and Rai, 2016; Waiyasusri et al., 2016). The quality of predicted results is strongly affected by the accuracy of the investigation of past and current trends, the data quality and the model applied for predictions (Mozumder and Tripathi, 2014). Over the years, several spatially explicit models have been developed and used successfully by integrating them with RS and GIS to simulate and predict future LULC scenarios such as Markov chain (MC) model (Muller and Middleton, 1994; Arsanjani et al., 2011; Fathizad et al., 2015), artificial neural network (ANN) model (Pijanowski et al., 2005; Mozumder and Tripathi, 2014; Maithani, 2015), cellular automata (CA) model (Clarke et al., 1997; Mitsova et al., 2011), logistic regression (LR) model (Kumar et al., 2014), GEOMOD (Giriraj et al., 2008; Paudel and Yuan, 2012), SLEUTH model (Jantz et al., 2004; Hua et al., 2014), conversion of land use and its effects (CLUE) model (Veldkamp and Fresco, 1996; Zhu et al., 2010). Every single model exhibits some advantages and disadvantages that have been described in detail by Triantakonstantis and Mountrakis (2012). The shortcomings of an individual model must be overcome by combining them to work as complementary to each other. Thus, in recent years various hybrid modeling methods have been developed and utilized successfully to predict liable patterns of future changes in LULC (Kamusoko et al. 2009; Arsanjani et al., 2013; Basse et

al., 2014; Mishra et al., 2014; Al-sharif and Pradhan 2014; Al-sharif and Pradhan, 2015; Bozkaya et al., 2015; Mishra and Rai, 2016). Although, the hybrid models provide the better and improved understanding of LULCC (Guan et al., 2011). But, it is very challenging to find out a hybrid model that provides the best result because each study offers a unique conclusion. Since the performance of LULCC modeling is different for different study area because of varied environmental conditions and landscapes of that individual area (Arsanjani et al., 2011). Thus, instead of identifying a single model, the best results providing model should be used for the study area. The comparison of models and prediction of the future LULC scenario using best result providing model are gaining more popularity in remote sensing community (Mas et al., 2014; Mozumder et al., 2016). Although, a substantial number of research using MC-based models exist, comparison studies are still limited. The present study aims to evaluate the performance of three MC-based hybrid models namely ST-MC, CA-MC and MLP-MC to simulate and predict future LULC scenarios in Varanasi district of Uttar Pradesh, India. More specifically, the objectives of the present study are to: (1) analyze the spatial and temporal patterns of LULCC in 1988-2001-2015; (2) Simulate and predict future scenarios of LULC based on ST-MC, CA-MC and MLP-MC; (3) determine the model that provides the better results in the study area; (4) predict future scenario of LULC for years 2030 and 2050 using the model providing best results.

7.2 STUDY AREA

Varanasi district of Uttar Pradesh, India is chosen for the present study. The area under investigation lies geographically between 25°10’ to 25°37’ N latitude and 82°39’ to 83°10’ E longitude covering an area of approximately 1532.91 km^2. The geographical location of the study area as viewed on Landsat 8-OLI image are shown in Figure 1.6.

7.3 MATERIALS AND METHODOLOGY

Three phases are involved in this work in order to model and predict the spatio-temporal dynamics of LULC in Varanasi district of Uttar Pradesh, India. The first phase involved the collection of remote sensing images covering the study area and the preparation of LULC layers for different years. The second phase involved the analysis of LULCC. In the third and final phase, the factors affecting the changes in LULC were determined, and the LULC based on past changes and the factors was simulated and predicted. For the present study, remote sensing images of Landsat 5-TM acquired on 04 November 1988, Landsat 7-ETM+ acquired on 31 October 2001, and Landsat 8- OLI image acquired on 15 November 2015 were used to produce LULC layers of Varanasi district of Uttar Pradesh, India. The details of multi-temporal remote sensing images used in this study are represented in Table 1.2. The SRTM DEM with 90 m spatial resolution was used to produce slope and aspect. The vector layer of roads and railway network was extracted from the Google Earth image. All the subsequent pre-processing, interpretation and LULC classification of multi-temporal remote sensing images were performed using ENVI (v 5.1) image processing software. Also, to model LULCC using three hybrid models which are ST-MC, CA-MC and MLP-MC, IDRISI Selva software has been employed as well as to predict the future LULC scenarios.

7.3.1 Pre-processing of remote sensing images

The collected multi-temporal remote sensing images were atmospherically corrected using QUAC module available in ENVI software and spatially referenced to a common UTM projection system (Zone 44, North) with datum WGS 84. All the images were resampled to the pixel size of 30 m. An appropriate band combinations are required to generate FCC for all the images. The band combination of B4, B3 and B2 was used to generate FCCs for

Landsat 5-TM and Landsat 7-ETM+ images. The band combination of B5, B4 and B3 was used to generate FCC for Landsat 8-OLI image. These FCCs were employed to create training samples (signatures) for LULC classification purpose. After the generation of training signatures, the separability analysis using transformed divergence (TD) method were used to examine the quality of training signatures prior to image classification. The separability analysis shows the range of values (from 1.75 to 2.0, where average divergence is 1.96) for Landsat-5 TM data of 1988, (from 1.75 to 2.0, where average divergence is 1.98) for Landsat-7 ETM+ data of 2001 and (from 1.76 to 2.0, where average divergence is 1.99) for Landsat-8 OLI data of 2015 respectively.

7.3.2 LULC classification and accuracy assessment

In this study, a supervised machine learning classification method support vector machine (SVM) was used to produce LULC maps for year 1988, 2001 and 2015 respectively. All the images were classified into seven major LULC classes: agricultural land, dense vegetation, sparse vegetation, fallow land, built up, water bodies and sand based on field investigation and landscape of the study area. The accuracy assessment of classification results was carried in terms of UA, PA, OA, Kc, and F-score based on confusion matrix using Equations (1.1) to (1.4) and (1.5).

7.3.3 Analysis of LULCC

The analysis of LULCC illustrates and quantifies the differences between the LULC of same the area at different years. The LULC maps based on classification of Landsat TM/ETM+/OLI images of years 1988, 2001, and 2015 respectively were used to quantify the LULCC within the study area. The changes occurred drastically affect the natural resources and environment. Thus, the recognition of changes and their causes would be helpful to

determine probable future changes and various LULC scenarios. The analysis and detection of LULCC is based on the changes in LULC classes from time 1 to time 2 (Eastman, 2009). In this study, cross-tabulation analysis was performed to quantify LULCC throughout 1988-2001 (period 1), 2001-2015 (period 2), and 1988-2015 (period 3) respectively. The gains and losses experienced by various LULC classes, contributions to net change in built up area and agricultural land, and analysis of spatial trend of change for built up area and agricultural land were also investigated within the study area for the period 1, period 2, and period 3.

7.3.4 Prediction of future LULC scenarios

In this work, three hybrid models namely ST-MC, CA-MC and MLP-MC were employed to model, simulate and predict the LULC scenarios to a specified future date. A brief description of hybrid models is given as follows:

7.3.4.1 ST-MC model

The MC is used as a stochastic process, that integrates each single category as the state of a chain (Weng, 2002). MC have been used broadly to model LULCC at large spatial scales (Muller and Middleton, 1994) using discrete state spaces. The first model applied in this work is ST-MC model because, it combines both the stochastic processes as well Markov chain analysis methods (Eastman 2009). This type of predictive LULCC model is appropriate when the past trend of a LULCC pattern is known (Eastman, 2009).

In the Markovian processes, the future state of a system can be predicted not based on the past but rather the present. In the beginning, MC generates a transition-probability matrix (Table 7.1), a transition area matrix (Table 7.2) and a set of Markovian conditional probability images (Figure 7.1) by analyzing LULC maps from two different dates (1988-2001) (Eastman 2009). After that a single LULC map for future prediction is produced by

aggregating all the Markovian conditional probability images. A stochastic choice decision model is used to perform this prediction. It generates a stochastic LULC map by assessing and combining the conditional probabilities in which each LULC can exist at each pixel location adjacent to a rectilinear random distribution of probabilities (Ahmed &Ahmed 2012).

Table 7.1 Markov transition probabilities of change among LULC (1988-2001) for 2015

LULC Class	Agricultural land	Dense Vegetation	Sparse vegetation	Fallow land	Built up	Water bodies	Sand
Agricultural land	0.1722	0.0811	0.3304	0.1471	0.2632	0.0057	0.0003
Dense vegetation	0.3185	0.1403	0.4581	0.0416	0.0318	0.0089	0.0008
Sparse vegetation	0.4396	0.1110	0.3147	0.0997	0.0278	0.0071	0.0001
Fallow land	0.4230	0.0845	0.3413	0.1218	0.0084	0.0148	0.0062
Built up	0.0365	0.0296	0.0389	0.0372	0.8293	0.0194	0.0091
Water bodies	0.0785	0.0520	0.1695	0.0857	0.0211	0.4669	0.1263
Sand	0.0591	0.0010	0.0618	0.2234	0.0010	0.2595	0.3945

Table 7.2 Transition area matrix (1988-2001)

LULC Class	Agricultural land	Dense vegetation	Sparse vegetation	Fallow land	Built up	Water bodies	Sand
Agricultural land	1060174	260787	1091732	372931	37290	20767	810
Dense vegetation	172386	75721	247299	22441	17138	4817	0
Sparse vegetation	978102	247028	700018	221868	61844	15746	172
Fallow land	347646	69466	280430	100088	6918	12198	5040
Built up	17446	4947	34768	7053	98705	3079	1260
Water bodies	12635	8380	27295	13804	3394	75175	20322
Sand	2694	46	2821	10190	46	11824	17994

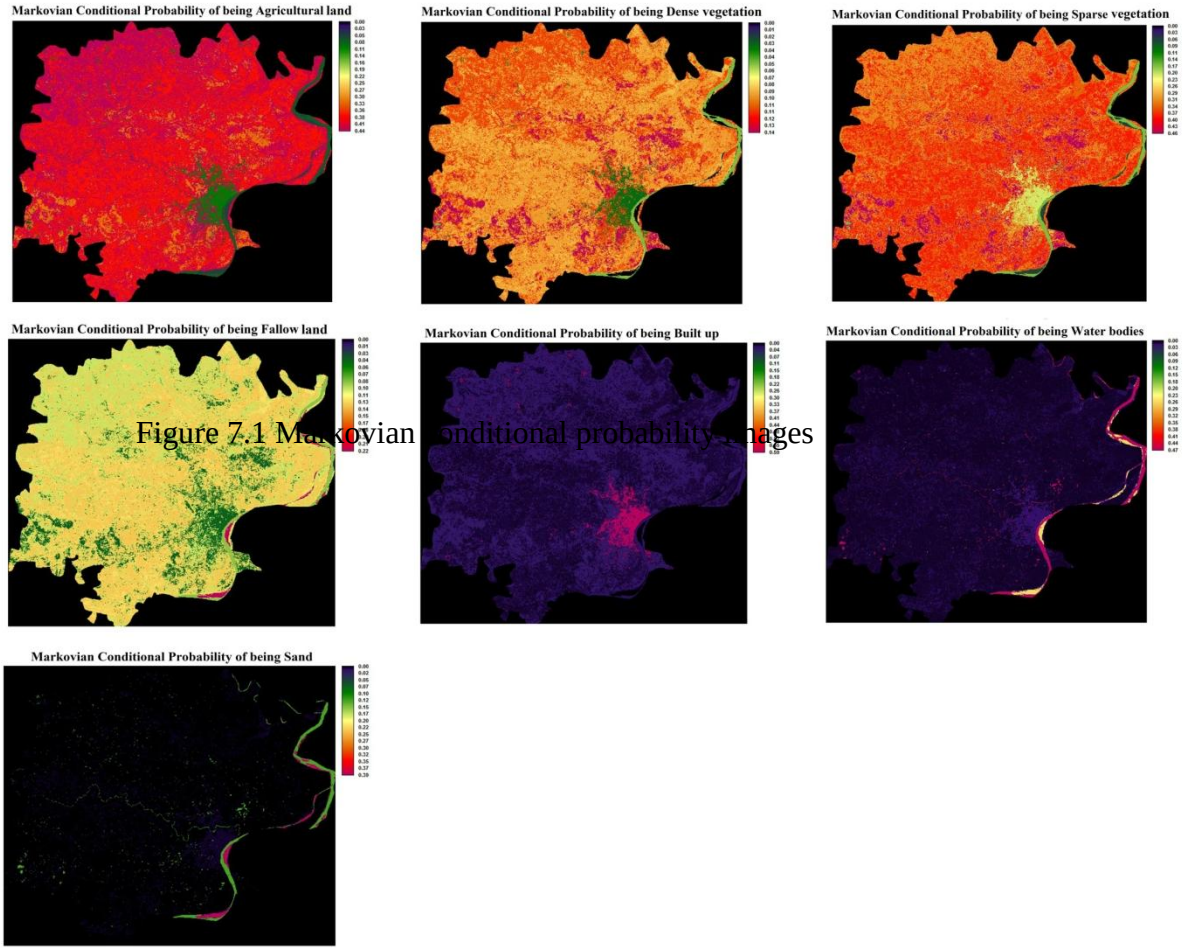

Figure 7.1 Markovian conditional probability images

Figure 7.1 Markovian conditional probability images

7.3.4.2 CA-MC model

CA-MC model binds the concepts of CA, MC, multi criteria evaluation (MCE) and multi objective land allocation (MOLA) (Eastman et al., 1998) resultant into a distinct dynamic model. Cellular automaton can be defined as an agent or object having the capability to change its state from a rule that describes the new state to its previous state and those of its neighbors. CA model is spatially dynamic in nature and commonly used for LULCC analysis and prediction (Adhikari and Southworth, 2012). The CA system consists of four components: cells, states, neighborhoods, and rules (Barredo et al., 2003). A cell is the smallest spatial unit and the cells immediately nearby to a certain cell are referred as the

neighborhood. The next state of each cell is established by the states of its neighborhood cells. The rules were used to describe the states of the cells for the future time step (Ahmed and Ahmed, 2012). In a CA model, the transition rule of a cell from one LULC to another is based on the state of the neighborhood cells (Verburg et al., 2004). The spatial component can be incorporated easily into CA, and simple rules are used by it to address dynamism with increased computational efficiency. The fundamental equation of CA model can be given as:

$$S(t, t+1) = f(S(t), N) \quad (7.1)$$

where S, t, t+1 and, N are the states of discrete cellular, the time instant, the next future time instant, the cellular field respectively and f represents the transition rule of cellular states in local space respectively.

The MC is a potential model for predicting land change demand when it is ambiguous to describe the changes and processes in LULC. It defines the future state of environment solely according to the previous state. MC model is a stochastic process that explains how likely one state is to transform into another and use it as the base to project changes in future. The critical attribute of the MC is the development of transition probability matrix of changes in LULC from time to time, which can be used to predict the future status through the analysis of past situations. Although it is convenient to model the changes, and determine the future trends using MC approach. But MC cannot be used solely for providing the information about the spatial allocation of these phenomena. Thus, the CA is utilized to describe the spatial components. In an integrated CA-MC model, CA deals with spatial dynamics using local transition rules while MC illustrates the temporal dynamics between LULC classes using transition probabilities (Eastman, 2006).

In this study, cellular automata analysis was carried out by the CA_Markov module in IDRIS Selva software. It uses a transition area matrix, a transition probability matrix and a set of transition probability maps showing the probability of each pixel to a specific LULC class. A transition probability matrix based on the cross-tabulation of two LULC maps of different years is produced and determines the probability of changing of a pixel from a LULC class into another class during that time epoch (Table 7.1). Also, a transition area matrix includes the number of pixels that are probable to change to a LULC class from another class during the time epoch (Table 7.2). Thus, a contiguity filter of 5×5 kernel size accounting the neighborhood pixels is applied to predict LULC from a time epoch to a later time epoch.

7.3.4.2.1 Generation of suitability maps for LULC classes

In CA-MC, it is required to determine the transition potentials to model the changes in LULC. The suitability maps are used as transition potential (Olmedo et al., 2013). The pixels that will change as per the highest suitability of each LULC class are determined by the suitability maps. If the suitability of a pixel is higher, the likelihood of the neighboring pixels to change into that particular class is higher. But it is complicated to prepare suitability maps for LULC classes in terms of data and information availability. Also, the incorporation of all types of factors or constraints that exist in the study area is not possible. Therefore, a fuzzy factor standardization procedure is assumed to be a simple assumption in this case. In suitability images values 0 and 255 show unsuitable and highly suitable respectively (Eastman, 2009). Therefore, in this case, a simple linear distance decay function is appropriate. In this study, multi-criteria analysis based on a fuzzy linear function was utilized to generate suitability images of the 7 for each LULC class and are shown in Figure 7.2. The

criteria of suitability maps were established by the observable pattern of past land transformation circumstances. The fuzzy linear function is a decision making process used to decide weights of selected criteria and constraints.

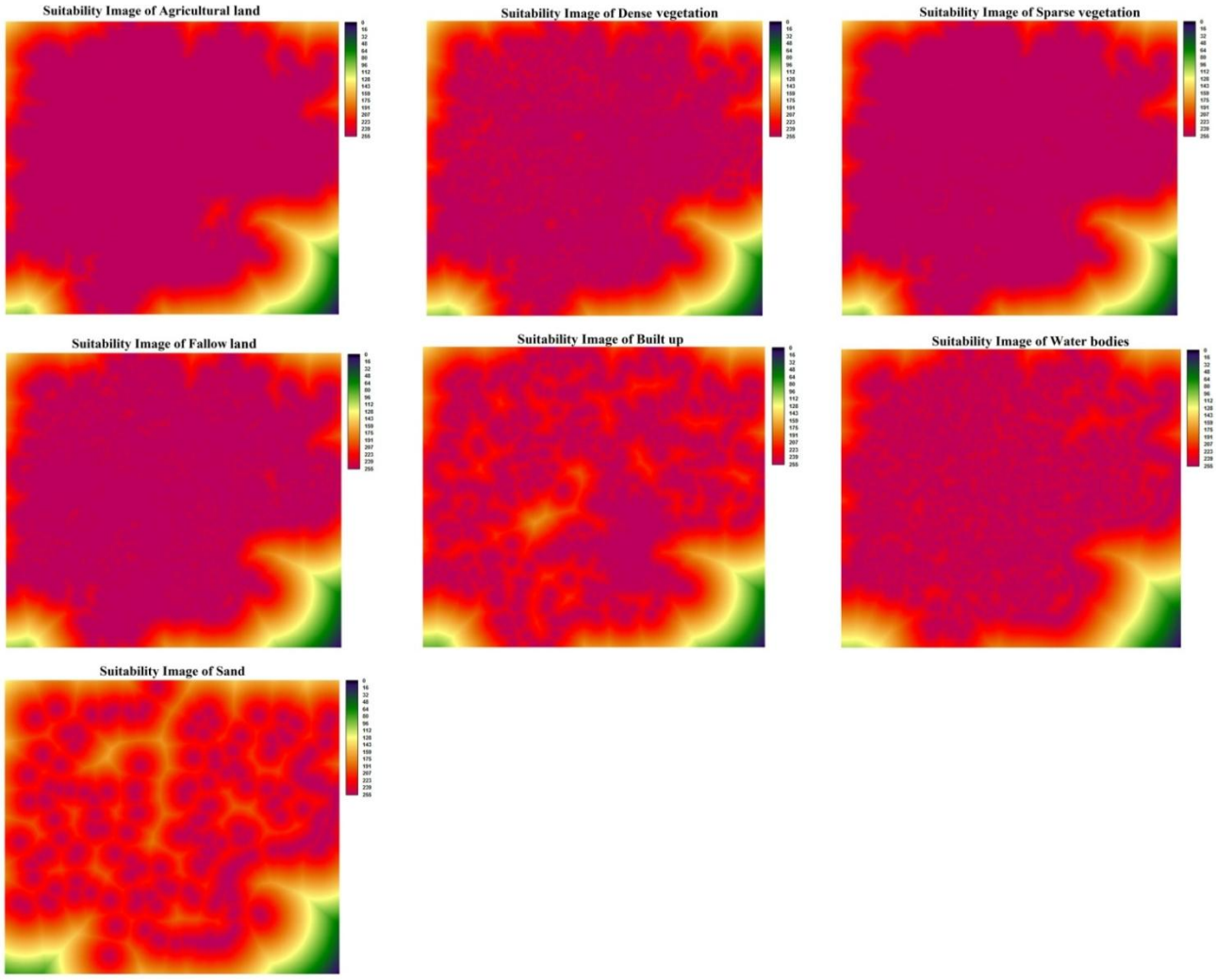

Figure 7.2 Suitability images of each LULC class

7.3.4.3 MLP-MC model

The world artificial neural network (ANN) is synonymic to the human brain (Mas and Flores, 2008). ANN has advantages over statistical methods because it does not assume probabilistic models of data. It can understand complex patterns present in the database, and model complex non-linear relationships (Ji, 2000; Atkinson and Tatnall, 1997). Although

many neural network models have been developed, the multi-layer perceptron neural network (MLPNN) is broadly used in different applications (Hu and Weng, 2009; Mozumder and Tripathi, 2014; Mishra et al., 2014). The MLPNN includes an input layer, many hidden layers and an output layer. One of the main advantages of MLPNN is its capability to model several or even all the transitions at one time. It is trained by supervised back propagation (BP) algorithm and provides the best generalization potential for transition of each LULC and simulation (Maithani, 2015; Mishra et al., 2014). It also combines the variables affecting the LULC transition (Mishra and Rai, 2016). The MC quantifies changes in LULC and determines transition probability areas to predict probable LULCC in the future (Dadhich and Hanaoka, 2011). In MLP-MC hybrid approach the transitions are modeled using an MLPNN. The integration of MLP and MC takes the advantages of both the models. A prediction model of future LULC scenario was designed within the MLP-MC structure available in the land change modeler (LCM) module embedded in IDRISI Selva software.

7.3.4.3.1 Selection of transitions and variables for model development

Since all the minor and major transitions occurred in LULC between two dates. Only the significant transitions that occurred among LULC classes were included in transition sub-model to improve the performance of MLPNN and get better results (Eastman, 2006). The possible factors driving LULCC in Varanasi district of Uttar Pradesh, India are characterized by nine major transitions: agricultural land to fallow land, agricultural land to built up, fallow land to agricultural land, fallow land to built up, dense vegetation to built up, dense vegetation to sparse vegetation, sparse vegetation to built up, sparse vegetation to fallow land, water bodies to sand. The transition potential was determined by developing sub-models in MLP-MC approach. All the observed LULC transitions were collected into a set of

sub-model. Each sub-model is added by significant variables either as static or dynamic (Eastman, 2006). A total of six environmental variables are considered in this study. Elevation, slope, and aspect were considered as static variables, while the distance from major roads, distance from rail network and distance from existing built up were regarded as the dynamic variable. An empirical likelihood to change map which is a qualitative variable was also produced besides these six quantitative variables. An empirical likelihood transformation is an effectual way of including categorical variables into the analysis. It is produced from the frequency of each LULC class occurred within the areas of transition (Eastman, 2009). All the seven explanatory variables used for the transition potential modeling are shown in Figure 7.3. Now, the potential explanatory power of these variables was tested using Cramer's V statistics. It is recommended that the variables having a Cramer's V of about 0.15 or higher are regarded as useful while those of about 0.4 or above are good (Eastman, 2009). After getting acceptable Cramer's V values for all the driving variables, now MLPNN model was run using BP algorithm.

The prediction results are also influenced by constraints and factors. The expansion of built up area is restricted by some criterions known as constraints. In the present study, major roads and rail network were considered as the constraints and shown in Figure 7.4. The region behind choosing the distance from major roads as a factor is that most of the construction and developmental activities are supposed to take place along the roads. Two model variables such as major LULC transitions and driving factors were previously defined. On the basis of this information, transition potential maps were created to visualize the suitability of LULC classes for its future scenario.

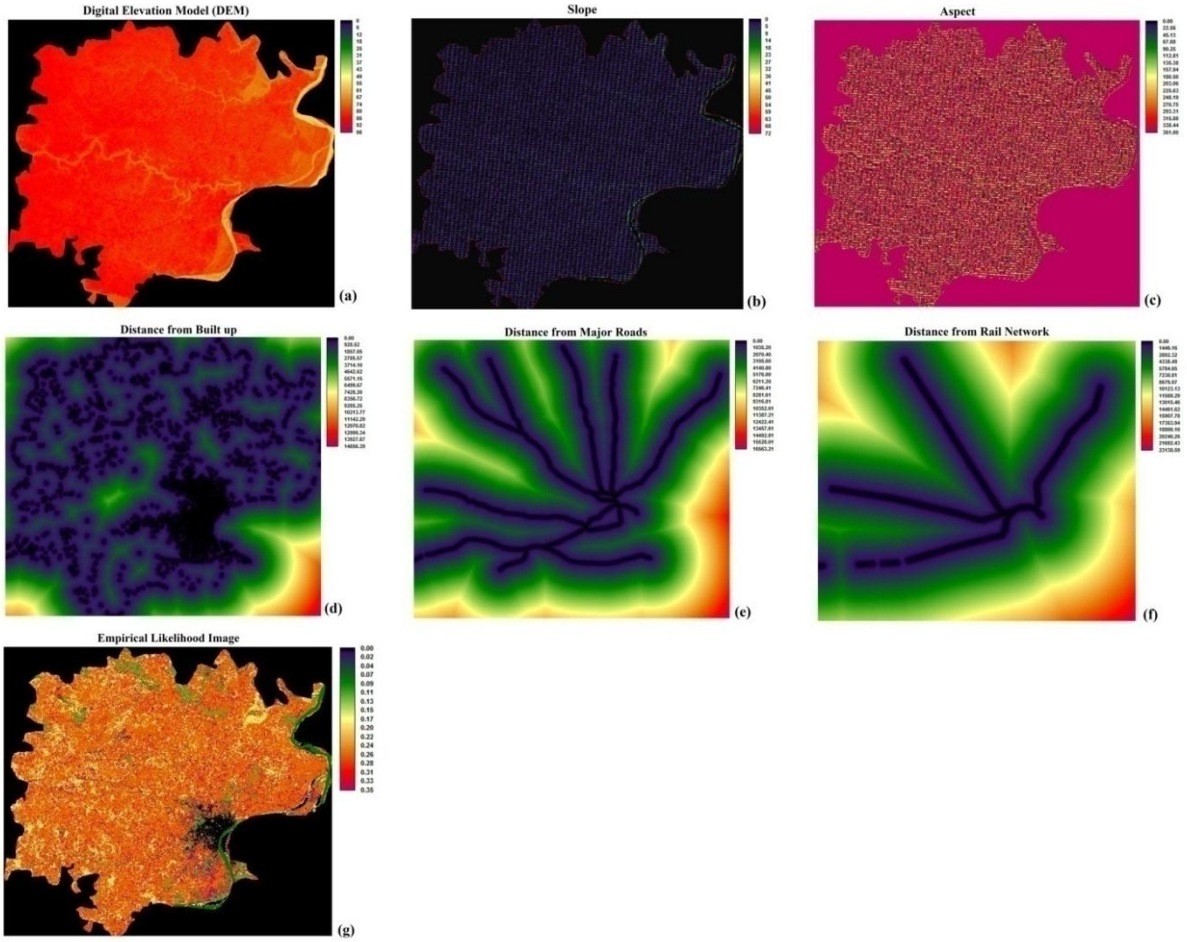

Figure 7.3 Explanatory variables (a) DEM, (b) slope, (c) aspect, (d) distance from built up, (e) distance from major roads, (f) distance from rail network, and (g) Empirical likelihood image

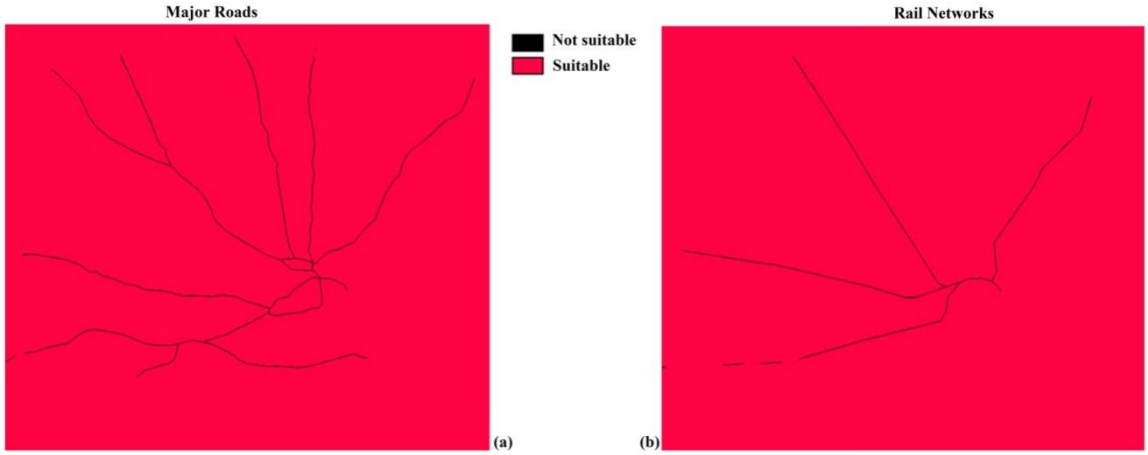

Figure 7.4 Constraints used (a) major roads, (b) rail network

7.3.4.3.2 Transition potential modeling

The transition potential maps were produced using seven variables as input, LULC transitions to be modeled and MLPNN integrated into LCM. The MLP first creates a random sample of cells that transitioned among LULC classes during the required time and starts the automatic training process. It keeps 50% of the samples for training and remaining 50% for testing the performance. In this study, the minimum number of cells that transitioned during 1988 to 2001 was chosen as 7959 to run MLP with 10,000 iterations. After running MLP, it was completed with an accuracy rate of 87.56% which is a measure of calibration. It is recommended that accuracy rate more than 80% is acceptable (Eastman, 2009). After the successful execution of MLP training, transition potential modeling is applied to generate transition potential maps. The amount of changes using the previous and later LULC maps were determined by MC process and used to estimate changes during the prediction process. The MC analysis also calculates the transition probability matrix of changing from one LULC class to other using past and current probabilities. Finally, the generated transition potential maps were further applied to predict LULCC scenarios for future dates. By using this information; transition potential maps were produced to visualize the suitability of LULC classes for future scenarios.

7.3.5 Validation of predicted results

If the evaluation of prediction provides convincing results, then the hybrid models can be applied further for the prediction of future LULC scenarios (Moghadam and Helbich, 2013). In general, the model validation is carried out by comparing the predicted and observed results. For this purpose, the LULC for the year 2015 was first predicted ST-MC, CA-MC and MLP-MC hybrid models based on LULC information from 1988 and 2001. The

predicted results were then compared with the actual LULC information observed by remote sensing image of 2015 with the help of kappa index statistics to test the validity regarding quantity and location (Kamusoko et al., 2009). The kappa index statistics includes the kappa for no information (K_{no}), kappa for grid-cell level location ($K_{location}$), kappa for stratum-level location ($K_{locationStrata}$) and kappa standard ($K_{standard}$) which is similar to kappa (Pontius, 2000).

7.4 RESULTS AND DISCUSSION

The results were divided into four components: (1) composition of the LULC maps and an accuracy assessment for the years 1988, 2001 and 2015; (2) change analysis of the period 1, period 2, and period 3; (3) prediction for the year 2015 by the ST-MC, CA-MC and MLP-MC models, and comparison of the prediction results with the observed LULC map of 2015, and identification of the model providing the highest accuracy for the study area; and (4) prediction of future scenarios of LULC for the year 2030 and 2050 using the best result providing model.

7.4.1 LULC maps and accuracy assessment

In this study, LULC maps of years 1988, 2001 and 2015 were produced based on SVM classifier. The quantitative and spatial distribution of different LULC for three different years 1988, 2001 and 2015 are shown in Table 7.3 and Figure 7.5 respectively. After the classification of multi-temporal remote sensing images, the obtained OA is the indicator of the reliability and usability of classified results. The PA, UA, OA, Kc and F-score achieved by confusion matrix approach are listed in Table 7.4. The OA of LULC maps for years 1988, 2001 and 2015 are 86.94%, 88.84% and 89.25%, respectively. The Kc for years 1988, 2001 and 2015 are 0.8475, 0.8697 and 0.8745, respectively. In this study, the accuracy assessment

of the classified products of the respective years confirmed that the results are acceptable for many applications.

Table 7.3 Area distribution of LULC of years 1988, 2001 and 2015

Year	1988		2001		2015	
LULC class	Area (km^2)	Area (%)	Area (km^2)	Area (%)	Area (km^2)	Area (%)
Agricultural land	965.86	63.01	873.78	57.00	909.83	59.35
Dense vegetation	86.64	5.65	121.54	7.93	65.94	4.30
Sparse vegetation	178.82	11.67	263.66	17.20	204.74	13.36
Fallow land	225.68	14.72	182.68	11.92	193.86	12.65
Built up	26.71	1.74	45.63	2.98	123.48	8.06
Water bodies	39.68	2.59	35.26	2.30	23.48	1.53
Sand	9.51	0.62	10.36	0.68	11.59	0.76
Total	1532.91	100	1532.91	100	1532.91	100

Table 7.4 Accuracy assessments of classified LULC maps of years 1988, 2001 and 2015

Year	1988			2001			2015		
LULC class	PA (%)	UA (%)	F-score (%)	PA (%)	UA (%)	F-score (%)	PA (%)	UA (%)	F-score (%)
Agricultural land	83.78	84.55	84.55	87.27	88.07	87.67	88.29	89.91	89.09
Dense vegetation	89.36	91.30	90.32	90.53	92.47	91.49	89.32	90.20	89.76
Sparse vegetation	86.61	87.39	87.00	87.16	87.16	87.16	88.39	90.00	89.19
Fallow land	84.91	79.65	82.19	85.98	81.42	83.64	85.71	84.96	85.33
Built up	88.29	90.74	89.50	89.09	91.59	90.32	88.99	88.99	88.99
Water bodies	88.35	94.79	91.46	91.58	96.67	94.05	92.39	94.44	93.41
Sand	87.76	81.90	84.73	90.83	86.84	88.79	92.71	87.25	89.90
OA (%)		86.94			88.84			89.25	
Kc		0.8475			0.8697			0.8745	

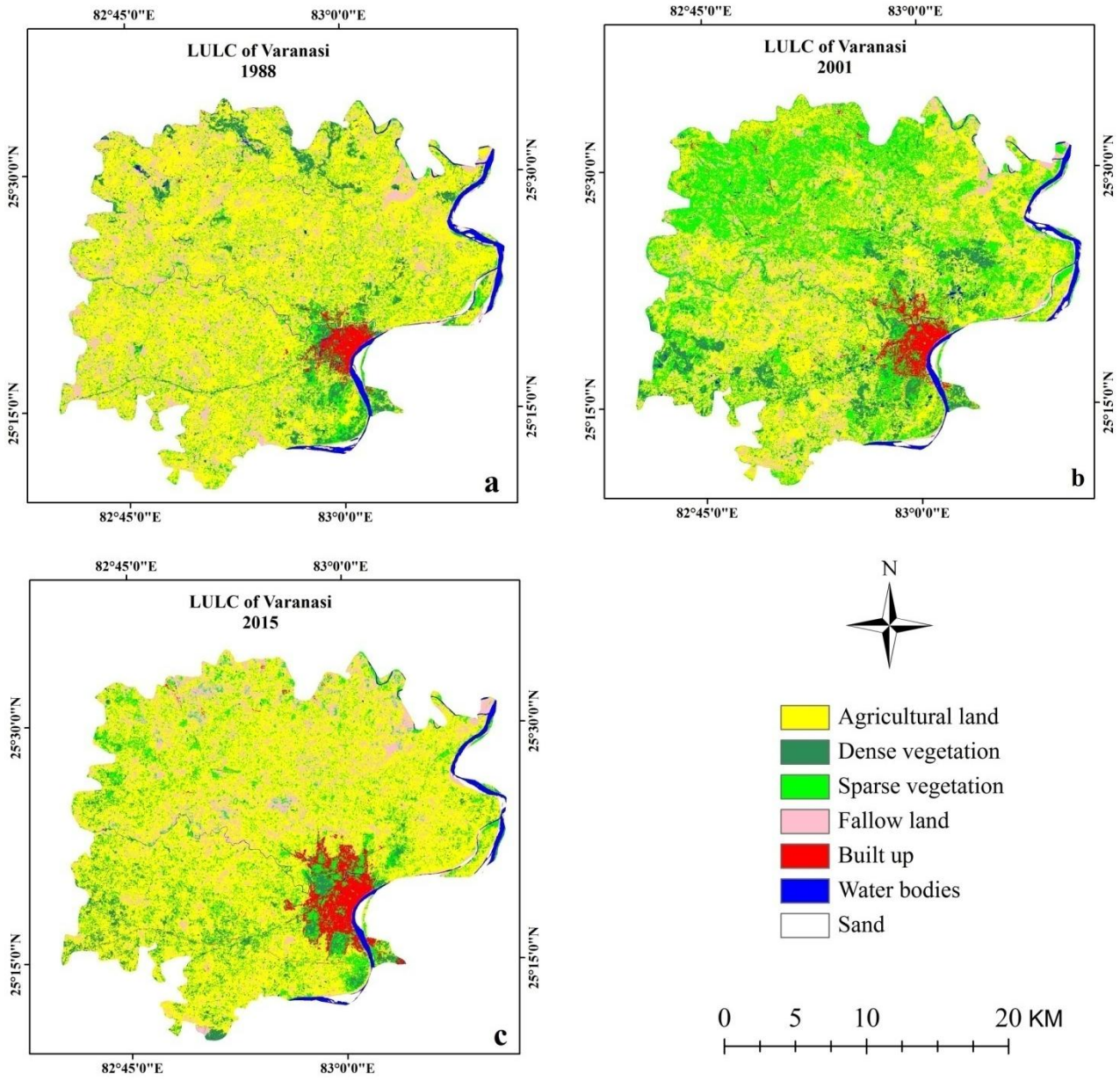

Figure 7.5 Classified LULC maps of years (a) 1988, (b) 2001, and (c) 2015

7.4.2 Analysis of LULCC

The study area experienced drastic changes in LULC and analyzed during period 1, period 2 and period 3. There are significant changes occurred in all LULC classes

particularly in agricultural land, fallow land, built up area and water bodies over the year (1988-2015).

The agricultural land in 1988 covered an area of 965.86 km^2 (63.01%), and it decreased to 873.78 km^2 (57.00%) and 909.83 km^2 (59.35%) in 2001 and 2015 respectively. During period 1 the agricultural land reduced by 6.01 %, while during period 2 it raised by 2.35% and during period 3 it again reduced by 3.66%. The area covered by dense vegetation in 1988 was 86.64 km^2 (5.65%) and it increased to 121.54 km^2 (7.93%) in 2001 while decreased in 2015 to 65.94 km^2 (4.30%). During period 1 the dense vegetation raised by 2.28%, while during period 2 it decreased by 3.63% and again decreased by 1.35% during period 3. The sparse vegetation covered an area of 178.82 km^2 (11.67%) in 1988 and it increased to 263.66 km^2 (17.20%) and 204.74 km^2 (13.36%) in 2001 and 2015 respectively. During period 1 the sparse vegetation raised by 5.53%, while during period 2 it decreased by 3.84% and again increased by 1.69% during period 3. The fallow land occupied an area of 225.68 km^2 (14.72%) in 1988 and it reduced to 182.68 km^2 (11.92%) and 193.86 (12.65%) in 2001 and 2015 respectively. During period 1 the fallow land reduced by 2.81%, while during period 2 it slightly increased by 0.73% and again reduced by 2.08% during period 3. It was examined that in 1988 built up covered an area of 26.71 km^2 (1.74%) and it increased to 45.63 km^2 (2.98%) in 2001 and 123.48 km^2 (8.06%) in 2015 respectively. The built up area raised by 1.23%, 5.08% and 6.31% during period 1, period 2 and period 3 respectively. The continuous decrease in water bodies is observed by 0.29%, 0.77% and 1.06 during period 1, period 2 and period 3 respectively. Sand is increased slightly by 0.06%, 0.08% and 0.14% during all the periods.

An enormous change of 6.31% in built up is observed between 1988 and 2015. Following this, there is a loss of 3.66%, 2.08% and 1.35% in agricultural land, fallow land, and dense vegetation respectively. The loss of agricultural land, fallow land and dense vegetation contributed to an increase in the built up between 1988 and 2015. This could be due to population growth linked with the requirement of land and urban supplies. The amount of changes in LULC during period 1, period 2 and period 3 are given in Table 7.5. The gains and losses of LULC classes during period 1, period 2, and period 3 are shown in Figure 7.6. The contributions to net change in built up and agricultural land during period 1, period 2, and period 3 are demonstrated in Figure 7.7 (a, b).

Table 7.5 Amount of changes in LULC during period 1, period 2, and period 3

	Amount of changes					
Period	1988-2001		2001-2015		1988-2015	
LULC class	Area (km^2)	Area (%)	Area (km^2)	Area (%)	Area (km^2)	Area (%)
Agricultural land	-92.08	-6.01	36.05	2.35	-56.04	-3.66
Dense vegetation	34.90	2.28	-55.59	-3.63	-20.70	-1.35
Sparse vegetation	84.83	5.53	-58.92	-3.84	25.91	1.69
Fallow land	-43.00	-2.81	11.18	0.73	-31.82	-2.08
Built up	18.93	1.23	77.85	5.08	96.78	6.31
Water bodies	-4.43	-0.29	-11.78	-0.77	-16.21	-1.06
Sand	0.85	0.06	1.22	0.08	2.07	0.14

During period 3, the rate of loss of water bodies is found maximum with -1.94% followed by dense vegetation with -1.01%, fallow land with -0.56% and agricultural land with -0.22%. The highest positive rate of change is found for built up to 5.67% followed by sand with 0.73%, sparse vegetation with 0.50%. It signifies that built up have the highest positive rate of change while the water bodies had highest negative rate of change during

period 3. The water bodies and dense vegetation with the higher negative rate of change may be a major concern in the study area. The complete information about the rate of change for each LULC class during period 1, period 2, period 3 is given in Table 7.6.

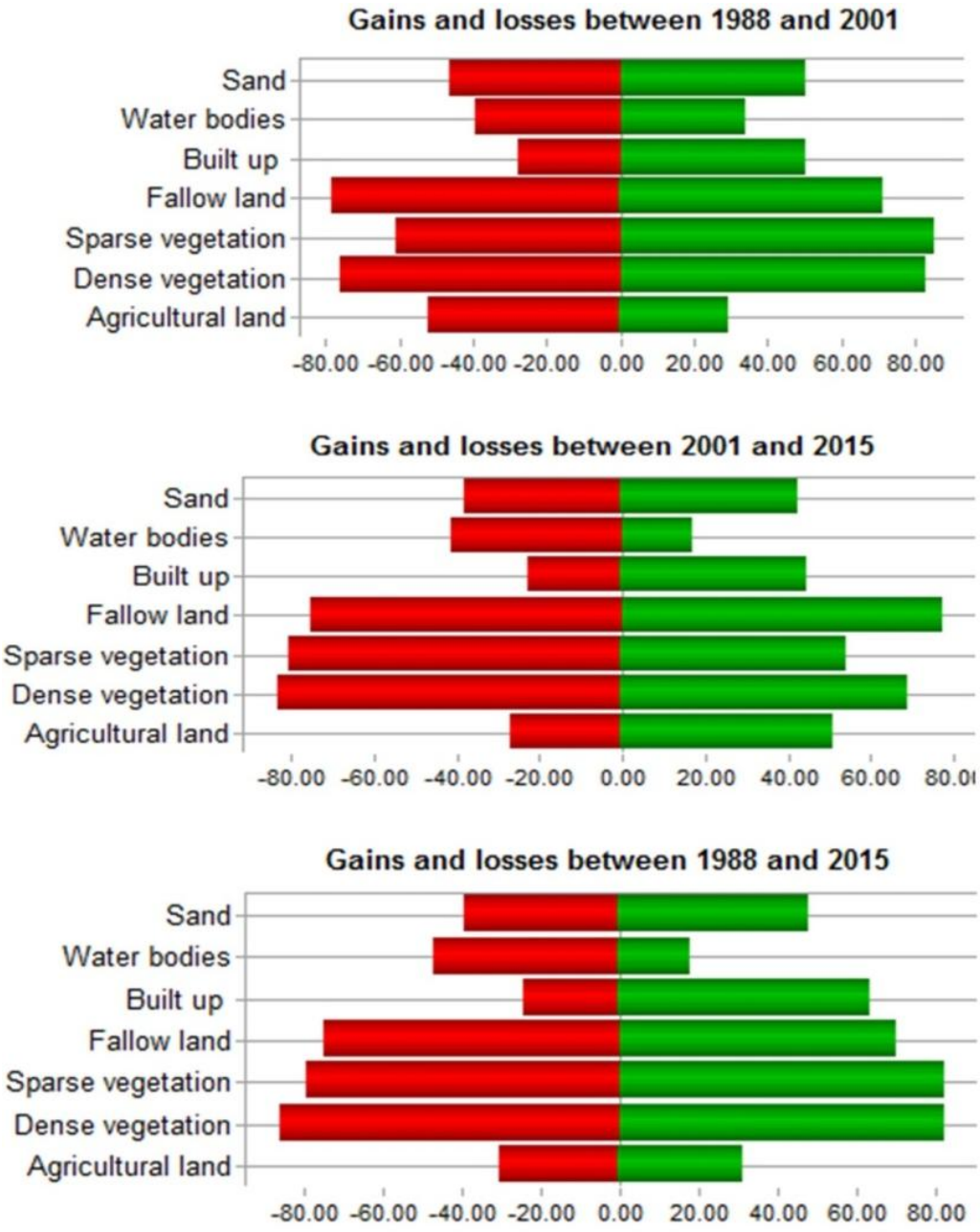

Figure 7.6 Gains and losses of LULC classes (in % change) during period 1, period 2, and period 3

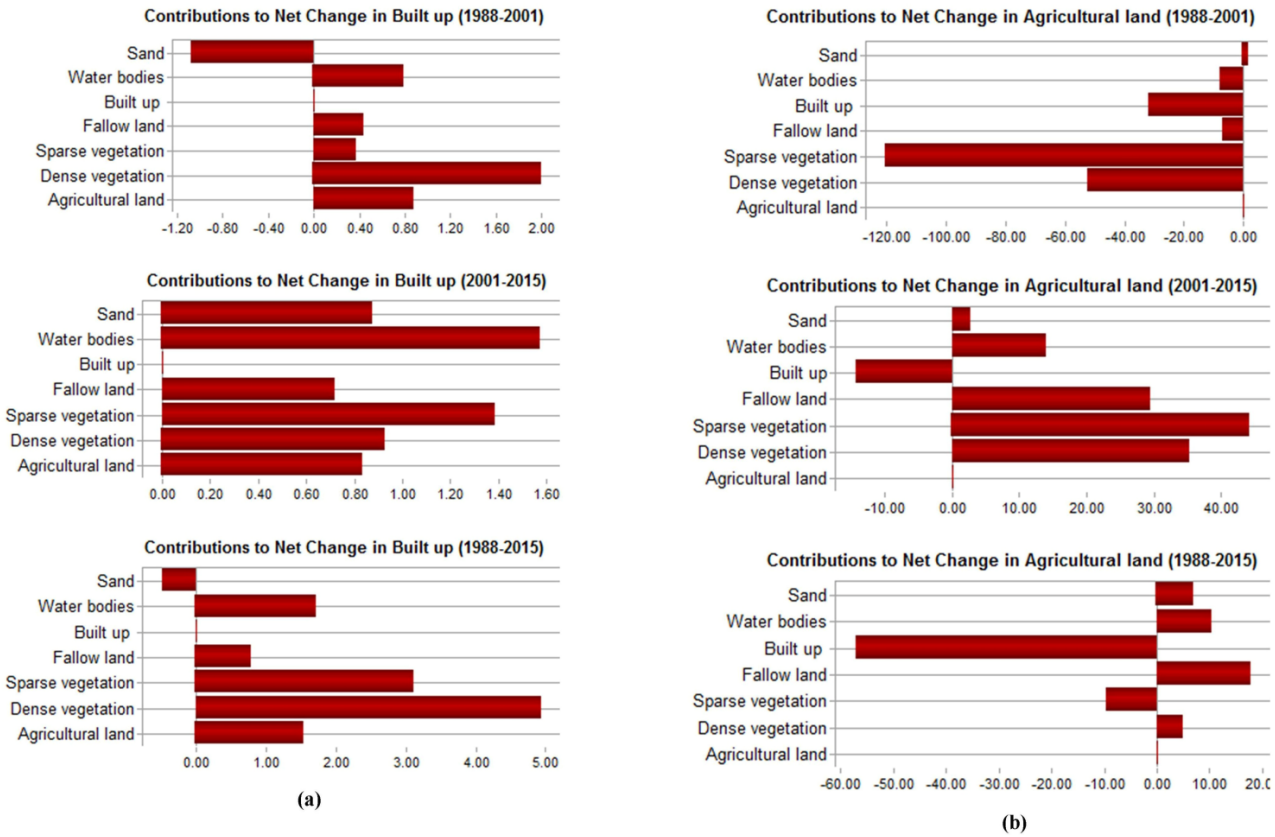

Figure 7.7 Contributions to net change in (a) built up and (b) agricultural land (in % change)

Table 7.6 Annual rate of change during period 1, period 2, and period 3

	Annual rate of change (%)		
Period	1988-2001	2001-2015	1988-2015
LULC class			
Agricultural land	-0.77	0.29	-0.22
Dense vegetation	2.60	-4.37	-1.01
Sparse vegetation	2.99	-1.81	0.50
Fallow land	-1.63	0.42	-0.56
Built up	4.12	7.11	5.67
Water bodies	-0.91	-2.90	-1.94
Sand	0.66	0.80	0.73

7.4.3 Spatial trend of change analysis

The spatial trend of change analysis is an effectual approach to visualize and provide the generalized patterns of changes by using two observed LULC maps of different years. The spatial trends of transitions from all LULC classes to built up and agricultural land during period 1, period 2, and period 3, respectively are shown in Fig. 7.8 (a- c). The spatial trend of change maps shows that the agricultural land is shifted towards the eastern and southern directions during all the periods. It is also observed that the transition of built up is more concentrated in the middle of the study area and expanding towards the northern and western directions during all the periods relative to other directions.

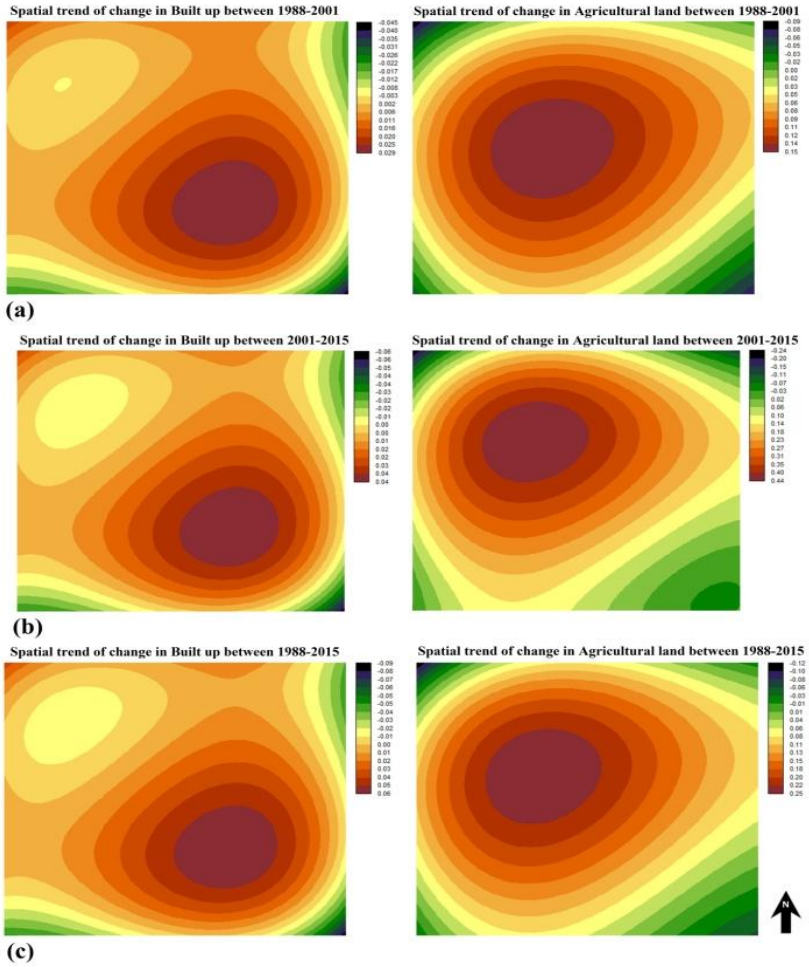

Figure 7.8 spatial trends of change in built up and agricultural land during (a) period 1, (b) period 2, and (c) period 3

7.4.4 ST-MC model based prediction

The prediction of future LULCC scenario was performed using a ST-MC model. Firstly, MC produces a transition probability matrix, a transition areas matrix and a set of Markovian conditional probability images by analyzing LULC maps of two different years 1988 and 2001(Eastman, 2009).

The transition probability matrix illustrates the probability that each LULC class will change to other classes in 2015. Markovian conditional probability images (Figure 7.1) are the probabilistic prediction based on the trends of past 13 years (1988-2001). The Markovian conditional probability of being built up ranges up to 0.59, which is highest among all other LULC classes. The probability values for agricultural land ranges up to 0.44, for dense vegetation ranges up to 0.14, for sparse vegetation ranges up to 0.46, for fallow land ranges up to 0.22, for water bodies ranges up to 0.47 and for sand ranges up to 0.39. Now by aggregating all the produced Markovian conditional probability images, a single LULC map for future prediction is generated.

7.4.5 CA-MC model based prediction

For predicting LULC map for the year of 2015, LULC maps of the years 1988 and 2001 were used to create the transition probability matrix. The suitability images were created by setting transition rules from one LULC class to another class. In this work, physical factors are only regarded as drivers of the changes in LULC. The physical proximity to an existing LULC class is assumed to be a driver of change into a specific LULC class in the future. The rules and suitability maps were prepared for each LULC classes. The fundamental supposition for producing suitability images is the pixel nearer to an existing LULC class has the higher suitability. In suitability images the values ranged from 0 to 255, 0 showing unsuitable and 255 showing highly suitable. Therefore, for this fundamental

supposition, a simple linear distance decay function is adequate. It provides the fundamental idea of contiguity and fuzzy set membership analysis procedure (Eastman, 2009) is used to standardize LULC maps to the same continuous suitability scale (0-255). Eventually, the prediction of LULC for year 2015 is carried out by utilizing the Markov transition area matrix, all the suitability images, the 5×5 CA contiguity filter and the LULC of 2001 as a base map.

7.4.6 MLP-MC model based prediction

The MLPNN analysis was used to determine the weights of transitions for the period of 1988 to 2001 that will be included in the transition probability matrix using MC analysis for future prediction. The transition probability matrix is the cross-tabulation of two LULC maps of different years (1988 and 2001) and shown in Table 7.7. In transition probability matrix rows and columns stand for the earlier and later date images. Based on all transition potential maps created for various LULC transitions, the MLPNN was applied with an accuracy of 87.56% with 10000 iterations.

Further, the Table 7.7 exhibits that the probability of change of agricultural land into built up in future date 2015 from 1988 to 2001 is 29.45 %, while the probability of changing of agricultural land into agricultural land in future is only 18.35 %. The probabilities of changing of agricultural land into built up raised up to 32.85 % and 33.55% in 2030 and 2050, respectively. Alternatively, the probabilities of changing of agricultural land into agricultural land in future dates reduced continuously to 16.52% and 15.85 % in 2030 and 2050, respectively. On the other hand, the probabilities of changing of agricultural land into built up increased remarkably from 29.45% to 32.85 and 33.55 % in 2030 and 2050 respectively. Markov transition probability matrices of changes among LULC for years 2030

and 2050 are given in Tables 7.8 and 7.9 respectively. It is notified through the quantitative and qualitative analysis of LULC maps of different years that there is rapid expansion of built up in Varanasi district of Uttar Pradesh, India which needs to be analyzed and modeled further.

Table 7.7 Transition probabilities of changes among LULC for Markov chain (1988-2001) for year 2015 in MLP modeling

LULC Class	Agricultural land	Dense Vegetation	Sparse vegetation	Fallow land	Built up	Water bodies	Sand
Agricultural land	0.1835	0.0751	0.3256	0.1145	0.2945	0.0065	0.0003
Dense vegetation	0.3104	0.1650	0.4445	0.0405	0.0308	0.0087	0.0001
Sparse vegetation	0.4041	0.1020	0.3702	0.0916	0.0255	0.0065	0.0001
Fallow land	0.4127	0.0825	0.3328	0.1433	0.0082	0.0145	0.0060
Built up	0.0289	0.0226	0.0451	0.0315	0.8546	0.0117	0.0056
Water bodies	0.0663	0.0440	0.1433	0.0725	0.0178	0.5494	0.1067
Sand	0.0523	0.0009	0.0547	0.1977	0.0009	0.2294	0.4641

Table 7.8 Transition probabilities of changes among LULC for Markov chain (2001-2015) for year 2030 in MLP modeling

LULC Class	Agricultural land	Dense vegetation	Sparse vegetation	Fallow land	Built up	Water bodies	Sand
Agricultural land	0.1652	0.0695	0.2967	0.1383	0.3285	0.0011	0.0007
Dense vegetation	0.2892	0.1602	0.4312	0.0683	0.0475	0.0034	0.0002
Sparse vegetation	0.3865	0.1051	0.3823	0.0927	0.0315	0.0017	0.0002
Fallow land	0.4311	0.0465	0.3422	0.1563	0.0114	0.0057	0.0068
Built up	0.0104	0.0118	0.0642	0.0281	0.8802	0.0038	0.0015
Water bodies	0.0694	0.0312	0.1264	0.0779	0.0216	0.5603	0.1132
Sand	0.0454	0.0001	0.0009	0.1708	0.0052	0.2129	0.5647

Table 7.9 Transition probabilities of changes among LULC for Markov chain (2001-2015) for year 2050 in MLP modeling

LULC Class	Agricultural land	Dense vegetation	Sparse vegetation	Fallow land	Built up	Water bodies	Sand
Agricultural land	0.1585	0.0759	0.2871	0.1421	0.3355	0.0007	0.0002
Dense vegetation	0.2852	0.1682	0.4529	0.0528	0.0371	0.0037	0.0001
Sparse vegetation	0.3952	0.1102	0.3916	0.0806	0.0205	0.0017	0.0002
Fallow land	0.4356	0.0309	0.3353	0.1494	0.0372	0.0061	0.0055
Built up	0.0248	0.0131	0.0504	0.0115	0.8953	0.0019	0.0030
Water bodies	0.0549	0.0292	0.1197	0.0595	0.0379	0.5795	0.1193
Sand	0.0496	0.0091	0.0062	0.1473	0.0108	0.2005	0.5765

7.4.7 Validation and selection of model

In this study, three MC-based hybrid models ST-MC, CA-MC and MLP-MC were used to predict future LULC scenarios. Three hybrid models were first compared to facilitate a valid prediction for future LULC scenario. The values of kappa index statistics for all three models are given in Table 7.10. It is clear from Table that $K_{no,}$ $K_{location}$, $K_{locationStrata}$ and $K_{standard}$ values for MLP-MC based predicted LULC map of 2015 are higher in comparison to that of CA-MC and ST-MC models. It is showing strong to perfect agreement between predicted and observed LULC maps because all values of kappa index statistics are greater than 0.80. The MLP-MC hybrid model provided the best results in comparison to other modeling methods for the study area. Finally, the future LULC scenarios were predicted quantitatively and spatially for 2030 and 2050 by better result providing MLP-MC model.

Table 7.10 Kappa index statistics for ST-MC, CA-MC, and MLP-MC based prediction results

Agreement	ST-MC	CA-MC	MLP-MC
K_{no}	0.7835	0.8581	0.8860
$K_{location}$	0.7977	0.8684	0.8948
$K_{locationStrata}$	0.7977	0.8684	0.8948
$K_{standard}$	0.7684	0.8302	0.8681

7.4.8 Prediction and analysis of future LULC scenarios for 2030 and 2050 using MLP-MC model

The LULC maps of 2001 and 2015 were used to predict the future LULC scenario for years 2030 and 2050 using MLP-MC model. By utilizing the LULC of 2015 as base map, transition potential maps, and the transition probability matrices of period 2001-2015, the future LULC scenarios were predicted for 2030 and 2050 as shown in Figure 7.9 (a, b). The resultant statistics of the area for various LULC classes are represented in Table 7.11.

Table 7.11.Area distribution of LULC of predicted years 2030 and 2050

LULC classes	Predicted 2030		Predicted 2050	
	Area (km^2)	Area (%)	Area (km^2)	Area (%)
Agricultural land	893.93	58.32	859.86	56.09
Dense vegetation	43.97	2.87	35.97	2.35
Sparse vegetation	161.83	10.56	132.83	8.67
Fallow land	185.86	12.12	205.86	13.43
Built up	215.68	14.07	269.68	17.59
Water bodies	20.76	1.35	18.76	1.22
Sand	10.89	0.71	9.96	0.65
Total Area	1532.91	100.00	1532.91	100.00

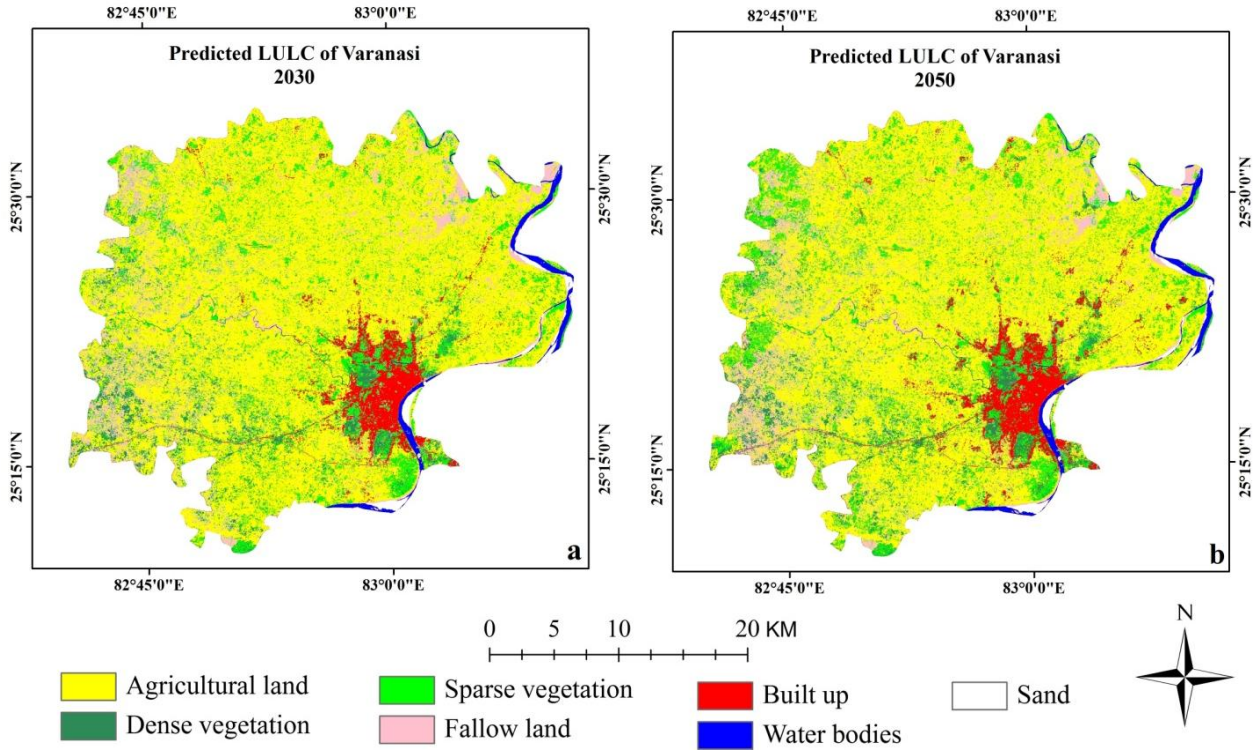

Figure 7.9 Predicted LULC maps of years (a) 2030, and (b) 2050

The MLP-MC based prediction result for 2030 showed that, there will be slight decrease in agricultural land (from 59.35% in 2015 to 58.32% in 2030), dense vegetation (from 4.30% in 2015 to 2.87% in 2030), sparse vegetation (from 13.36% in 2015 to 10.56% in 2030) and fallow land (from 12.56% in 2015 to 12.12% in 2030). While increase in built up (from 8.06% in 2015 to 14.07% in 2030). Nevertheless, prediction result for 2050 showed that it would experience the decrease in agricultural land (from 59.35% in 2015 to 56.09% in 2050), dense vegetation (from 4.30% in 2015 to 2.35% in 2050), and sparse vegetation (from 13.36% in 2015 to 8.67% in 2050). While, increase in fallow land (from 12.56% in 2015 to 13.43% in 2050) and built up (from 8.06% in 2015 to 17.59% in 2050). The overall loss of agricultural land and sparse vegetation occurred because of the rapid spreading of built up area. While slight changes were showed by other LULC classes during 1988-2050. These

results propose a worrisome change for the future scenario of the landscape of Varanasi district of Uttar Pradesh, India. Therefore, it deserves attention regarding sustainable management and development of the landscape.

7.5 CONCLUSION

In this study, a combined approach of satellite remote sensing images, GIS and prediction models was explored to understand the spatio-temporal dynamics of LULC and its future scenario in Varanasi district of Uttar Pradesh, India. For this purpose, LULC patterns were examined by using Landsat TM/ETM+/OLI images of respective years 1988, 2001 and 2015. After that, the future LULC scenarios were predicted for 2015 using ST-MC, CA-MC and MLP-MC hybrid models respectively in the study area. The validation of prediction models was assessed using observed LULC map of 2015 with the help of kappa index statistics. Based on validation results, the MLP-MC model pointed out a descriptive capability of future prediction and found more appropriate in comparison to CA-MC and ST-MC models.

The prediction results for 2030 showed an increase of 92.20 km^2 in built up whereas the slight decrease of 15.90 km^2 in the agricultural land between 2015 and 2030. Furthermore, the prediction results for 2050 showed an increase of 146.20 km^2 in built up whereas decrease of 49.97 km^2 in agricultural land between 2015 and 2050. The analysis of LULCC between1988-2050 demonstrated that there is a vast increase in built up while a considerable reduction in agricultural land, dense vegetation and sparse vegetation.

In this study, multiple simulation models were used to realize the future LULC prediction more accurately. Comparison of three different models enabled the recognition of prediction results using the better performing model for the study area. However, the

accuracy of prediction results is strongly related to many factors. Firstly, the accuracy of LULC maps and the prediction results are negatively affected by the moderate resolution of multi-temporal Landsat images. Second, it is assumed to have uniform transition probability in the Markov chain model. It is still not easy to include the unpredictable influence of other variables, like government policy or socioeconomic aspects. So, to achieve improved results, image quality should be increased, and new prediction models should be developed by incorporating more socio-economic and physical variables.